

A High Performance PWM Voltage Source Inverter Used for VAR Compensation and Utility Grid Stability Improvement

Azeddine Draou¹

Department of Electrical and Electronics, College of Engineering/ University of Hail, Saudi Arabia

ABSTRACT: A high performance advanced static VAR compensator (ASVC) which uses a Pulse Width Modulation (PWM) voltage source inverter is presented and analyzed in this paper. A fast control approach of the ASVC system has been implemented for applications that require leading or lagging power compensation. The proposed control strategy is based on an explicit control of the reactive power, implicit of the voltage amplitude of the capacitor of the dc side and is more flexible. The analysis of the simulation results, inserted in this paper, reveal the technical feasibility of using such an ASVC to improve the stability of the infinite bus system and allow us to conclude that the use of the inverter as compensator of reactive power brings better performances than classical ones.

Keywords: VAR Compensation. PWM inverter, ASVC, Control, Utility Grid, Stability

I. INTRODUCTION

The requirement to design and operate power systems with highest degree of efficiency, security, and reliability have been central focus for the power system designer, ever since the interconnected networks came into existence. To satisfy these requirements, various advances in technology of AC power transmission have taken place in the context of effective control of reactive power and its compensation [1].

In the past, synchronous condensers, mechanically switched capacitors and inductors, and saturated reactors have been applied to control the system voltage in this manner[1,2]. Since the late 1960s, thyristor controlled reactor (TCR) devices together with fixed capacitor or thyristor switched capacitor have been used to inject or absorb reactive power[3,4]. The controllable series compensator such as the thyristor controlled series compensation (TCSC) has been developed to change the apparent impedance of a line by either inductive or capacitive compensation, facilitating active power transfer control. It suffers from the disadvantages that it generates low order harmonic components into the power system. Recently, voltage source converter has been developed to operate as static VAR compensators [5-7]. Such compensators are dynamic reactive power compensation devices which use a voltage source inverter transforming a DC component to AC through a capacitor seen here as a power storage device. They have also the advantage of reduced size and weight, precise control and very fast response. The advanced static VAR compensator i.e. known as ASVC may resemble the operation of synchronous condensers but in a static manner. The converter supplies reactive power to the network by increasing the synthesized inverter output voltage. And similarly, it absorbs VARs from the network by reducing the output voltage below the network voltage, i.e., no large power components such as capacitor banks or reactors are used. Only a small capacitor is employed to provide the required reference voltage level to the inverter. The possibility of PWM voltage source converters with high switching frequency for reactive power compensation is also reported [8,9]. In this paper, the operating principles of the advanced static VAR compensator (ASVC) which is developed in this work is based on the technique of the exact equivalence with the conventional rotating synchronous compensator. The ASVC system has been modeled using the d-q transform. Computer simulation results are provided and discussed to validate the performance of the proposed model.

II. REACTIVE POWER PHENOMENA

2.1 Reactive Power in Electrical Systems

In order to enhance the quality of the power and energy in the grid transmission system we have to control the reactive power by usually compensating individual or group of loads. Moreover, the voltage and frequency must be constant everywhere and display a pure sine wave and a near unity power factor, and must be independent of the size and kind of the consumer loads. This can only be achieved by inserting reactive power compensators and may lead to a better power factor correction; improvement of the voltage regulation; and a good load balancing [14-15].

2.2 Classical Solutions for Compensating the Reactive Power

Classical reactive power compensators are an essential part of the power system in order to minimize transmission losses, maximize power transmission capability, and maintain the supply voltage. In the following, a brief description of some of these classical compensators is given:

- Synchronous compensator: the cost of such system is high and encumbering [16].
- Bank of capacitors are generally designed for compensating parameters that vary slowly, usually fractioned so to adjust the reactive power to be compensated.
- The thyristor-Switched capacitor type of compensator consists of switching on and off capacitors by using static switches. It may be slow since equating the supply-capacitors voltages will lead to a delay in the action.
- Thyristor controlled reactor is constituted of an inductance supplied through an AC-AC converter made of two thyristors in anti-parallel. In general TCR is associated with batteries so that it can absorb or supply reactive power.

- Figure 1 shows the typical method of static VAR compensation. The leading reactive current necessary for VAR compensation is actually supplied by connecting capacitor banks across the AC lines. A capacitor bank connected in this way is called a thyristor switched capacitor (TSC).

2.3 Proposed Advanced Static VAR Compensator

After introducing classical methods for compensating the reactive power, we propose a new concept of the advanced static var compensation [10] based on the exact equivalence with the classical rotating synchronous compensator. This type of compensator uses a source voltage type inverter with a capacitor in the DC side used as energy storage element. The dynamic behavior of the system in open loop will be the key of the synthesis of such an approach of control, and it will be shown that this control approach is more efficient for industry applications [11-13]. The major ASVC system component is a three phase PWM forced commutated voltage source inverter as shown in Figure 2. The ac terminals of the inverter are connected to the ac mains through a first order low pass filter. Its function is to minimize the damping of current harmonics on utility lines. The dc side of the converter system is connected to a dc capacitor, which carries the input ripple current of the inverter and is the main reactive energy storage element. The dc supply provides a constant dc voltage and the real power necessary to cover the losses of the system. Figure 3 shows a simplified equivalent circuit of the ASVC. In this representation, the series inductance L_s accounts for the leakage of the transformer and R_s represents the active losses of the inverter and transformer. C is the capacitor on the dc side. The inverter is assumed to be loss less. V_{oa} and V_{sa} are the amplitude of the fundamental of the output voltage of the converter and phase voltage of the supply, respectively. The operating principles of the ASVC can be explained by using its phasor diagram. When the amplitude of the inverter output voltage V_{oa} is smaller than the supply voltage V_{sa} , the reactive power is absorbed by the ASVC. Otherwise, the ASVC generate the reactive power when the amplitude of the supply voltage is larger than the output voltage of the inverter.

III. BEHAVIOR ANALYSIS OF THE ASVC SYSTEM

To achieve an easier modeling of the system, the original circuit is subdivided in several basic sub-circuits as shown in Figure 3. Detailed analysis are given in [18]. Collecting all parts of the system, while introducing the model of the dc part in the system, the complete mathematical model of the ASVC in d-q axis will be as follows:

$$\frac{d}{dt} \begin{bmatrix} i_q \\ i_d \\ v_{dc} \end{bmatrix} = \begin{bmatrix} -\frac{R_s}{L_s} & -\omega & 0 \\ \omega & -\frac{R_s}{L_s} & \frac{m}{L_s} \\ 0 & \frac{m}{C} & 0 \end{bmatrix} \begin{bmatrix} i_q \\ i_d \\ v_{dc} \end{bmatrix} + \frac{V_s}{L_s} \begin{bmatrix} -\sin\alpha \\ \cos\alpha \\ 0 \end{bmatrix} \quad (1)$$

From equation system (1), we can extricate the expressions for i_d , i_q , v_{dc} . Expressions of real and reactive power are given by:

$$p_c(p) = v_{sq}i_q + v_{sd}i_d = -V_s(i_q \sin\alpha - i_d \cos\alpha) \quad (2)$$

$$q_c(p) = v_{sq}i_d - v_{sd}i_q = -V_s(i_d \sin\alpha + i_q \cos\alpha) \quad (3)$$

3.1 The ASVC behavior in steady state

Equations governing the steady state behavior of the ASVC can be obtained by equating the term of derivatives in the mathematical model given by equations (1) to zero, which comes to similarly having to short-circuit inductors and to open the capacitor. We note that the active and reactive power depend only on the square of the supply voltage and the resistor of coupling of the ASVC to the ac mains, and independent of the other parameters of the circuits (L_s and C).

In addition, the dc side voltage depends on α , the modulation index, and the resistor and inductor of the coupling, but independent of the value of the dc capacitor. While the system parameters are given by: Supply: $V_s = 220$ V, $f = 50$ Hz,

$$R_s = 1\Omega, \quad L_s = 5 \text{ mH} \quad \text{DC side : } C = 50\mu\text{F}, \quad m = \frac{1.12}{\sqrt{3}}$$

By varying the angle α in an interval of -30° to $+30^\circ$ which is the linear zone for sine and cosine, we obtain the following responses.

Figure 4 shows that i_q , i_d and v_{dc} values for different values of α , where we can note that the real current i_d is always zero, on the other hand the reactive current i_q and the dc voltage v_{dc} are linear according to α .

3.2 The ASVC behavior in transient state:

Taking as an initial condition for the DC side voltage, the maximum voltage of the supply, a series of dynamic responses of the system to step changes of $\pm 10^\circ$ of the angle α have been established [16]:

Figure 5 shows the response of the reactive current i_q to a step change of $\alpha = -10^\circ$, which after a short transient state attains a stable value of 38 A supplied to the network.

Figure 6 shows the response of the active current i_d , $\alpha = -10^\circ$ which after the voltage v_{dc} reaches its stable value, it goes to zero, because its action on the transient state is only for charging and discharging the DC side capacitor.

3.3 Programmed PWM generation pattern

Two methods of PWM generating pattern were thoroughly investigated and the method which offers better voltage utilization and lower switching frequencies thus less stress on switching devices and reduction of the switching losses was used in the paper. The set of non linear equations might be solved by the method of Newton Raphson. The expressions of the slopes are :

$$m_p = 5.0391e^{-0.07125M}$$

$$m_n = -6.4384e^{-0.05672M}$$

Hence, we give the approximations of the angles of initial commutation as a function of the modulation index as :

$$\alpha_K = m_p IM + c_K \quad K = 1, 2, 4, \dots etc.$$

$$\alpha_K = m_n IM + c_K \quad K = 3, 5, 7, \dots etc.$$

with :

$$\text{for } MI = 0 \quad c_1 = 0 \quad c_2 = \frac{120}{(M + 1)}$$

$$c_K = c_{K+1} = \frac{(K + 1)60}{M + 1}$$

$$c_{M-2} = \frac{(M - 1)60}{M + 1} \quad 3 \leq K \leq M - 2, K \text{ odd}$$

$$\text{et } c_{M-1} = 60 \quad c_M = \frac{(M + 3)60}{M + 1}$$

For our case, we took $M=11$, that is to eliminate the harmonics having the following order : 5, 7, 11, 13, 17, 19, 23, 25, 27, and 29.

Hence, Figure 7 shows the trajectories of the angle of commutations for modulation index varying between 0 to 1.15.

Figure 8 shows the switching pattern, and the corresponding line to neutral output inverter voltage.

The switching angles of the programmed PWM pattern are obtained by the resolution of a set of nonlinear equations as shown in [8], [9].

A programmed PWM switching pattern which allows the elimination of selected number of harmonics [1] is continuously applied to the six controlled switches. This method is used because it offers better voltage utilization and lower switching frequencies thus less stress on switching devices and reduction of the switching losses (increase of the efficiency of the converter).

The parameters of the programmed PWM pattern used in this paper are given by: MI (modulation index) = 1.12

3.4 Controller design [18]

The controller design of the ASVC is based on the linearized model of the system under some assumptions such as disturbance α_Δ being small, the second-order terms are dropped, and the quiescent operating α_0 is near zero. Thus the PI controller is conceived so that the ASVC has a desired dynamic performance. The PI transfer function is: The closed loop transfer function of PI associated to the transfer function of the ASVC is given by:

$$[F_{PI}.G]_{BF}(p) = \frac{F_{PI}.G}{1 + F_{PI}.G} \quad (4)$$

The parameters of the PI controller can be shown to be:

$$K_p = K = 7.5 \cdot 10^{-6}$$

$$K_i = \frac{K}{T_i} = 2.5 \cdot 10^{-3}$$

IV. CONTROL STRATEGY AND PERFORMANCE ANALYSIS OF THE PROPOSED ASVC

3.1 Proposed control block diagram

Figure 9 shows the main control circuit of the system, it represents the different blocks constituting the control system. The source voltage and the ASVC's currents are transformed in the d-q axis for calculating the reactive power generated by the system which is compared to the reference, the vector PLL detect the phase angle of the supply which is added to the control variable α (output of the PI controller). This sum adjusts the reading frequency of the counter connected to the EPROM where switching pattern is stored.

3.2 Simulation results of the ASVC acting alone

To verify analytical key results and the validity of the proposed control scheme [16], the aforementioned ASVC structure was tested on Pentium personal computer. Computer simulation was carried out using Mat lab, with the system

parameters given by: Supply: $V_s = 220\text{ V}$, $f = 50\text{ Hz}$, $R_s = 1\Omega$, $L_s = 5\text{ mH}$; Dc side : $C = 500\ \mu\text{F}$; PI controller : $K_p = 7.5 \cdot 10^{-6}$, $K_I = 2.5 \cdot 10^{-3}$

Testing of the ASVC system shown in Figure 9 was performed for dynamic response. The amplitude of the reference was adjusted to cause the system to swing from leading to lagging mode.

Figure 10 shows the simulated reactive power response to a reference change from 10 kVar lagging to 10 kVar leading.

Performance evaluation of the subject model has also been tested for current and voltage responses to step changes.

Figure 11 shows the simulated current and voltage waveforms to a step reference change from 10 kVar lagging to 10 kVar leading, this figure confirms that the compensator time response is fast (about 10 ms).

3.3 Application of the advanced static VAR compensator for the improvement of stability of a turbo alternator

Recent developments in the solid state VAR compensators have opened a very optimistic door towards achieving a very efficient control of reactive power. This stems from the fact that the voltage is maintained constant within a specified level, to improve the dynamic stability of the power system and its power factor as well as correcting the phase unbalance. In this section, we will study the case when disturbances occur at the studied machine without affecting the behaviour of the other machines that is (speed and E.M.F are constants). This means that the voltage and frequency of the network can be considered constants. The turbo-alternator is then connected to a distribution network called 'infinite'.

3.3.1 Proposed control strategy of the network-ASVC

Based on Figure 12 we can establish various equations [19], hence our model will be made up of ten differential equations, seven for the alternator and three for the ASVC. For the initialisation of the system, we take for the machine the same conditions given in [16], and for the ASVC the following initial conditions:

$$v_{dC} = \frac{\sqrt{2} v}{m}$$

$$i_{dC} = 0$$

$$i_{qC} = 0$$

Figure 12 shows the main principles of the proposed control of the ASVC, the reactive power demanded is always compensated partly by the capacitive reactive power generated by the ASVC, this method of compensation help ease the alternator and increase the security boundary for the heating of the rotor circuit. The reactive power demanded being inductive must be compensated by a capacitive reactive power generated by the ASVC. A PI regulator controls this compensation, which synthesizes the control variable α which is added to the angle δ that is necessary for synchronizing with the voltages of the bus bar considered. This sum being α_c is applied to the ASVC to generate the necessary reactive power; the control variable α being limited by two upper and lower levels will allow preserving the stability of the compensator. If we suppose that the reference is always the voltage of the bus bar connected to the ASVC, the transfer function relating the reactive power to the control angle α is given by [17]. As for the PI regulator, it is designed similarly as given in section 29.3.5 with the same constant of time of integration, but the voltage level will change. Hence by using the root locus method, the parameters of the regulator are given as follows:

$$K_p = 2.3 \cdot 10^{-9}$$

$$K_I = 7.7 \cdot 10^{-7}$$

3.3.2 Simulation results

To further demonstrate the usefulness of the proposed ASVC, we used it with a turbo alternator to analyze the performance of its stability. A series of simulation tests have been carried out and will be given below. To analyze the performance of the stability of the turbo-alternator with ASVC, a series of simulation tests have been carried out, by taking the compensator parameters as follows: AC side : $R_s = 1\Omega$, $L_s = 5\text{ mH}$; DC side : $C = 500\ \mu\text{F}$.

Figure 13 represents the variation of the load angle of the turbo alternator group with and without compensation after clearing the fault of 0.08 s, we notice that the response with the compensation is more damped and the load angle is smaller than that of the turbo alternator without compensation.

Figure 14 represents the variation of the voltage of the first bus bar with and without compensation, the voltage of the system compensated is higher than that without compensation, this is due to the decrease in reactive power in the lines by the ASVC which generates a capacitive reactive current which annuls a part of the inductive reactive current absorbed by the line.

Figure 15 shows the variation of the load angle of the turbo-alternator with and without compensation after the clearing of the fault of 0.3 s, which is the critical time for clearing the fault for the alternator without compensation. We notice that the introduction of the ASVC has allowed to improve this clearing time and to increase the level of stability of the system.

V. CONCLUSION

A new model of advanced static VAR compensator has been developed. A fast control approach of the ASVC system has been implemented for applications that require leading or lagging power compensation. The proposed control strategy is based on an explicit control of the reactive power, implicit of the voltage amplitude of the

capacitor of the dc side and is more flexible. The simulation results show that this control strategy has good dynamic performances for generating or consuming of the reactive power. In this paper a new approach to improve the stability of a turboalternator using a static VAR compensator has been presented. The proposed system has been analyzed and a fast current controller been implemented for reactive power applications. The mathematical model derived and the transient simulated results obtained are included to confirm the applicability of the proposed control scheme.

REFERENCES

1. H. S. Patel, and R. G. Hoft, "Generalized Technique of Harmonic Elimination and Voltage Control in Thyristor Inverters: Part I- Harmonic Elimination", IEEE Trans. on Ind. Appl. Vol. IA-9, pp. 310-317, May / June 1973.
2. S. R. Bowes, R. R. Clements, "Computer aided design of PWM inverter systems", IEE. Proc., Vol. 129, Pt. B, N°1, January 1982.
3. H. Akagi, Y. Kanazawa, A. Nabae, "Generalized Theory of The Instantaneous Reactive Power in Three - Phase Circuits" IPEC, Tokyo'83, pp1375-1386.
4. H. Akagi, Y. Kanazawa, A. Nabae, " Instantaneous Reactive Power Compensators Comprising Switching Devices Without Energy Storage Components " IEEE Trans On Ind. Appl. Vol. IA-20, N° 3, May/June 1984.
5. H. W. Van der Broeck, H.-CH. Skudelny, G. Stanke, "Analysis and Realization of a Pulse Width Modulator Based on Voltage Space Vectors", Proc. of IAS'86, 1986, pp. 244-251
6. P. N. Enjeti, J. F. Lindsay, " Solving Nonlinear Equations of Harmonic Elimination PWM in Power Control ", IEEE Trans. Ind. Appl. Electronics Letters Vol. 32, No 12, 4th June 1987.
7. L. Moran, P. D. Ziogas, and G. Joos, "Analysis and design of a Synchronous Solid-state Var Compensator", IEEE Trans. on Ind. Appl. Vol. IA-25, No 4, July / Aug. 1989, pp.598-608.
8. P. N. Enjeti, P.D. Ziogas, and J. F. Lindsay, " Programmed PWM Techniques to Eliminate Harmonics: A Critical Evaluaton", IEEE Trans. Ind. Appl. Vol. 26, No 2, March / april 1990.
9. G. Joos, L. Moran, and P. D. Ziogas, "Performance Analysis of a PWM Inverter VAR Compensator", IEEE Trans. on Power Electronics, Vol. 6, No 3, July 1991, pp. 380-391.
10. L. Gyugi, "Unified Power-Flow Control Concept for Flexible AC Transmission Systems", IEE. Proced. C, Vol. 139, N°4, July 1992.
11. D. R. Trainer, S. B. Tennakoon, R. E. Morrison, " Analysis of GTO-based Static VAR Compensators " IEE Proc.-Electr. Power Appl., Vol. 141, No 6, November 1994.
12. J.B. Ekanayake ., N.Jenkins. , N.B. Cooper. : 'Experimental investigation of an advanced static Var compensator'. IEE Proc.-Gener. Transm. Distrib., Vol. 142,No.2, March 1995.
13. A. R. Bakhshai, G. Joos, H. Jin, " Space Vector Pattern Generators for Multi-Module Low Switching Frequency High Power Var Compensators", Proc. of PESC'97, 1997, pp.344-350.
14. H. Akagi, Fellow, IEEE, "The State-of -the -Art of Power Electronics in Japan",IEEE,Trans.Power.Electr. Vol.13, No. 2. 1998
15. G.C.Cho, G.H.Jung, N.S. Choi, and G.H. Cho, Member, IEEE, Analysis and Controller Design of Static Var Compensator Using Three-Level GTO Inverter, *IEEE Trans. Power Electron.* Vol.11, no. 1, jan 1996, 111-111.
16. T. J. E. Miller, " Reactive Power Control in Electric Systems ", John Wiley and Sons, Inc. 1982.
17. M. H. Rashid, *Power Electronics: Circuits, Devices, and Applications* (Prentice Hall, Englewood Cliffs, Inc. 1994).
18. A. Tahri, M. Benghanem and A. Draou, "A Non-linear Control and Modelling of an Advanced Static Var Compensator", International Conference on Electronics, ICEL'98, 5-7 October 1998, U.S.T.Oran, Algeria, pp 209-213.
19. A. Draou, M. Benghanem, A. Tahri, and L. Kotni, 'A New Approach to Modelling Advanced Static Var Compensator', Conf. Rec IEEE/CESA Vol.3, No.7, pp.573-578, Hammamet, Tunisia, April 1998.

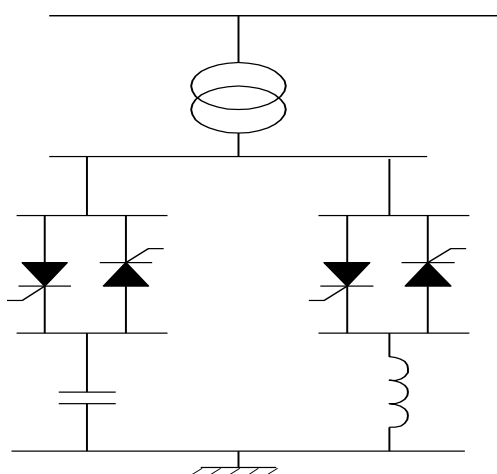


Fig.1 Static VAR compensation using TSC and TC

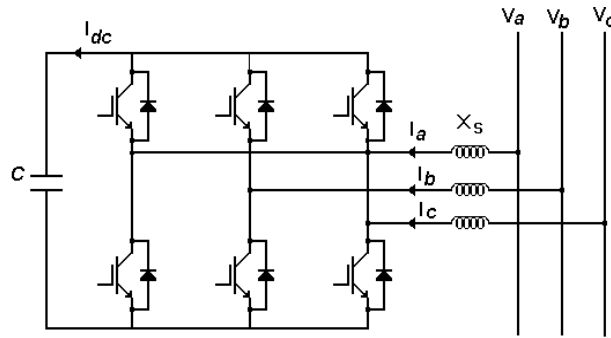


Fig.7 Main circuit of ASVC

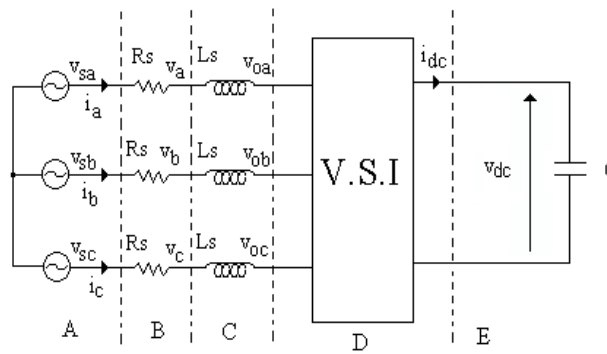


Fig.3 Equivalent circuit

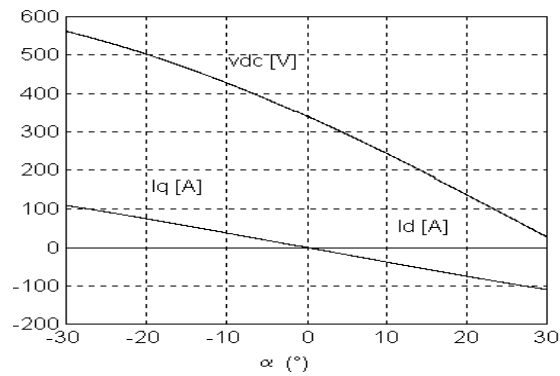


Fig.4 Steady state values

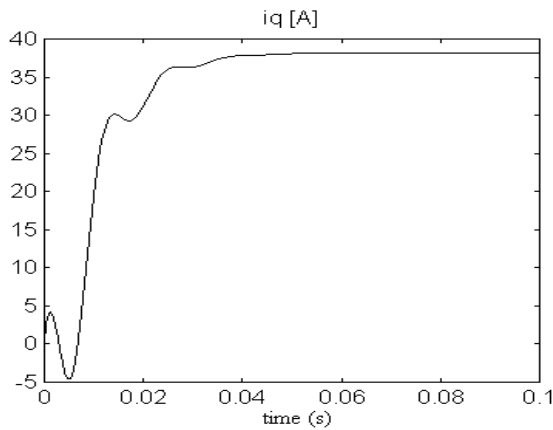


Fig.5 Transient reactive current response

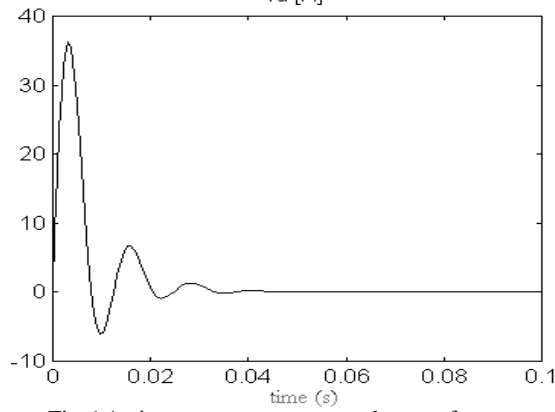


Fig.6 Active current response to change of m

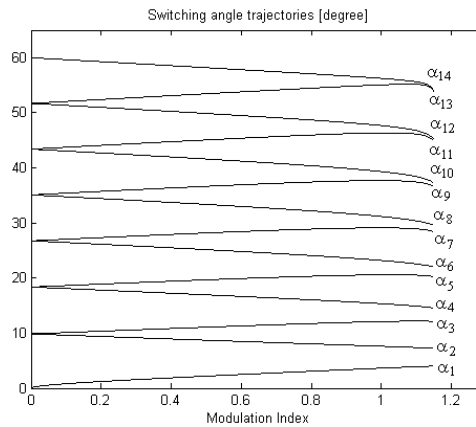


Fig.7 Switching angle trajectories for eliminating 13th harmonics

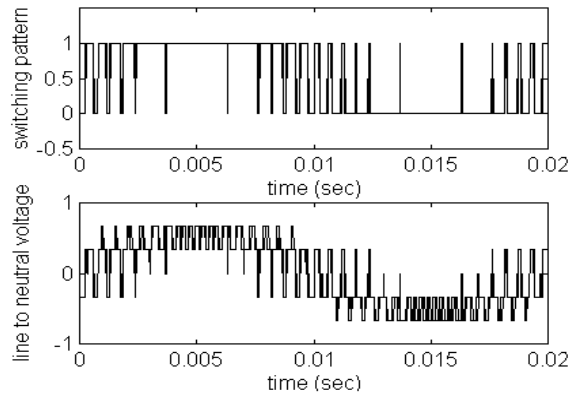


Fig. 8 Switching pattern and line to neutral

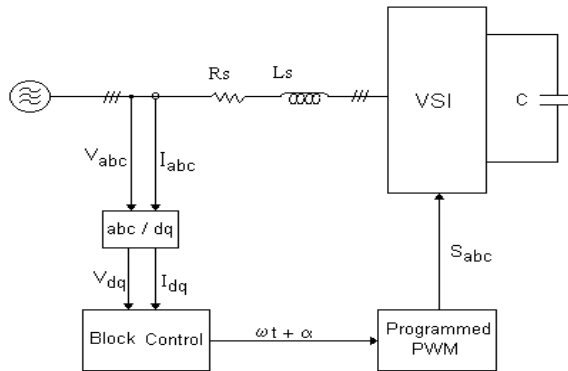


Fig.9 Main and control circuit of the proposed system.

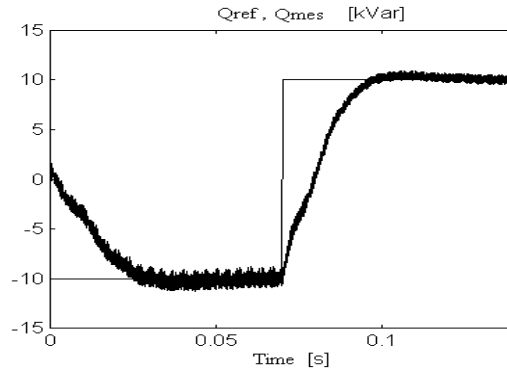


Fig.10 Simulated reactive power response

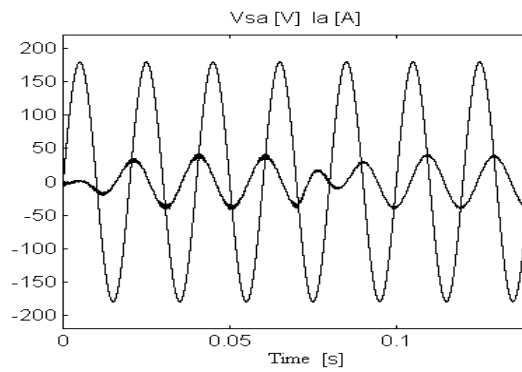


Fig. 11 Simulated current and voltage waveforms

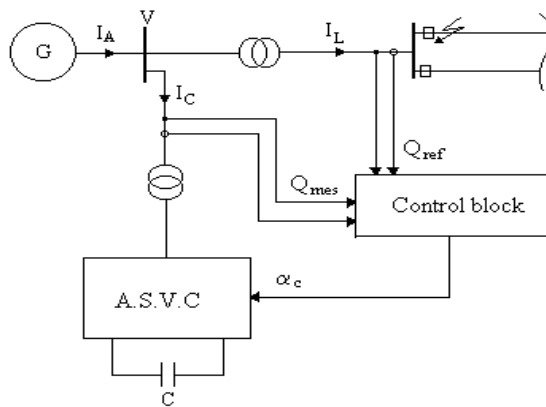


Fig.12 Main circuit configuration of the proposed system

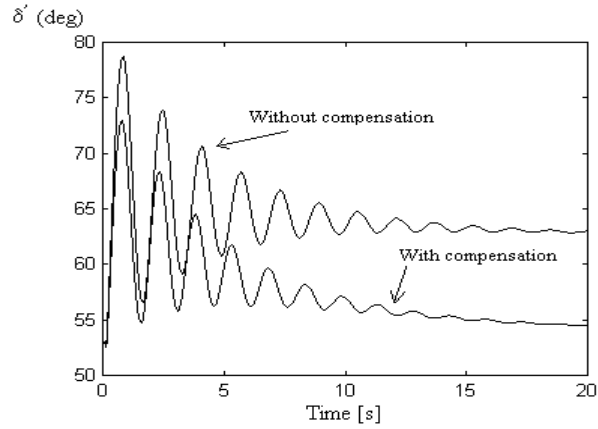


Fig.13 Load angle variation

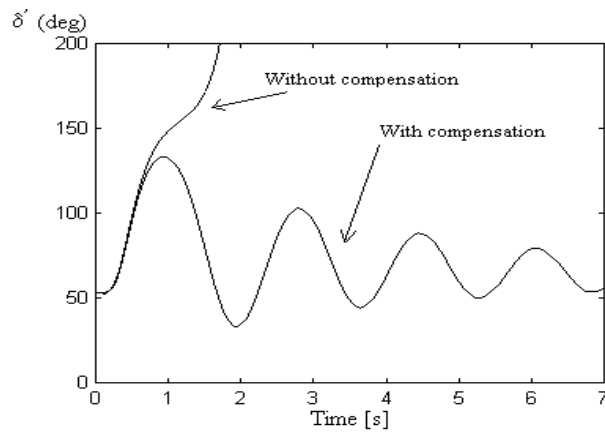


Fig. 14 Variation of the voltage of the first busbar

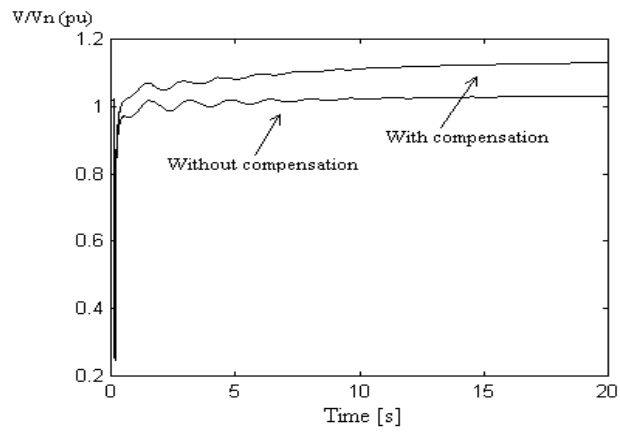


Fig. 15 Variation of the load angle of the turboalternator